INVESTIGATIONS INTO THE 'PELLINI' DROP-WEIGHT TEST FOR CHARACTERISING STRUCTURAL CRACK ARREST BEHAVIOUR

C S Wiesner* and S D Smith*

Previous work has demonstrated that there exists an empirical correlation between the nil-ductility transition temperature (NDTT) and structural crack arrest behaviour. The present work comprises three-dimensional elastic-plastic finite element analysis of the 'Pellini' specimen geometry and instrumented drop-weight tests to study the mechanics of this test, and to reconcile the correlation with fracture mechanics principles. It is shown that the existing correlation can be explained in terms of a consistent stress intensity factor at crack arrest in both drop-weight specimens and in large-scale, structurally representative crack arrest tests. The findings enhance the confidence in the drop-weight test as a measure of structural crack arrest behaviour.

INTRODUCTION

The prevention of failure by avoiding brittle fracture initiation can be complemented by crack arrest considerations. These are particularly useful where failure initiation cannot be precluded, but instead, an arrested brittle crack is shown to be safe. The crack arrest approach can therefore provide additional confidence where accidental overloads may occur (1).

Crack arrest properties can be determined using small-scale fracture mechanics test specimens (2) or large-scale, structurally representative, wide plate tests, e.g. Ref.3. Previous work (4,5) has found an empirical correlation between the crack arrest temperature (CAT) and the nil-ductility transition temperature (NDTT) determined using 'Pellini' drop weight test (DWT) specimens, see Fig.1a. The CAT is the temperature above which crack arrest is very likely for a given applied stress (typically ½ to ⅔ the yield strength) and crack length (typically around 100mm). There is also evidence (7) that the NDTT correlates well with crack arrest toughness (K_{Ia}) transition temperature determined using compact crack arrest tests. An analytical approach could further substantiate these empirical correlations. Some analytical work (e.g. 8-10) on DWT specimens has been carried out, but proved inconclusive.

* TWI, Abington Hall, Abington, Cambridge, UK

In the present study, three-dimensional elastic-plastic finite element analyses of a cracked DWT specimen have been carried out. In addition, tests were carried out using instrumented specimens loaded both statically and dynamically, to obtain the mechanical conditions at the instant of crack initiation and arrest. The steel investigated was a 25mm thick normalised C-Mn plate to BS4360:1990 Grade 50EE, with a NDTT = -65°C.

FINITE ELEMENT ANALYSIS OF CRACKED DROP-WEIGHT SPECIMEN

The finite element model of the 19mm thick (P2) DWT specimen is shown in Fig.2. The model was loaded in three point bending to simulate the impact roller test displacement of 1.5mm. The computations were carried out using the general purpose finite element code ABAQUS (11).

One of the problems when modelling the drop-weight specimen configuration is the ill-defined crack shape. Based on preliminary tests and literature data (10), it was decided to use the limit of the HAZ of the weld bead crack starter to define the shape of the crack, as this is a well-defined and realistic representation of the arrested crack shape when testing specimens in the temperature range (NDTT +30°C) to (NDTT +40°C).

The DWT is a go/no go test (i.e. generally the crack either arrests when it emerges from the brittle crack starter or it penetrates into the test material). This means that the crack arrest toughness inferred from the applied stress intensity factor for the crack size defined above is a 'greater than' estimate. The present analysis is not intended to replace conventional crack arrest toughness values, but rather to give an estimate of the arrest toughness from the drop-weight test results.

For the elastic-plastic calculations, the dynamic stress/strain curve determined at a strain rate of about $8.3s^{-1}$ was used, corresponding approximately to the strain rates encountered in DWTs. Although the increase of yield strength due to dynamic loading was taken into account, it should be noted that the present FEA results are based on static analyses, and did not account for the dynamic DWT loading. In addition, crack driving forces in actual DWT specimens are influenced by welding residual stresses originating from the weld bead which were not considered in the present analysis.

The computed stress intensity factor, K, was calculated from the J-integral using the plane stress relation $K_J = (JE)^{0.5}$. The values are plotted versus the normalised distance from the tension face, i.e. along the crack front, in Fig.3. The results in Fig.3 show that the elastic analysis predicts a higher stress intensity factor at the tension surface than at the deepest point of the crack. This behaviour has also been observed for penny shaped surface cracks in tension or bending and is likely to be intensified due to the presence of the weld bead. However, this analysis result does not reflect the true crack driving force in a drop-weight specimen since it will be subject to plastic deformation at the tension surface. Furthermore, examination of fracture faces (see Fig.1b) shows that the actual crack propagation in drop-weight tests does not take place along the tension surface but rather in the depth direction.

A more uniform stress intensity factor distribution is achieved from the elastic–plastic analysis (solid symbols in Fig.3). Nevertheless, the stress analysis still results in a slight increase of the stress intensity factor at the tension face of the specimen, in contrast with experimental crack propagation paths. However, Fig.3 represents the stress state when the specimen hits the deflection stops, i.e. after a displacement of 1.5mm. As will be seen below, crack initiation and arrest in DWTs normally take place before this displacement is reached.

The stress intensity factor at the tension surface and at the deepest point of the specimen are plotted as a function of the specimen displacement in Fig.4. This figure shows that the stress intensity at the deepest point exceeds the value at the tension surface for displacements of less than 0.7mm. Thus, when crack initiation and arrest take place before or around this value of specimen displacement, the experimental observation that crack propagation takes place preferentially in the depth direction (Fig.1b) is in agreement with the FEA results.

The important result of the finite element analysis of a P2 DWT specimen with a HAZ crack shape is that the applied effective stress intensity factor in the cracked specimen lies between 70 and 150MPa$\sqrt{m}$ (Fig.4) for specimen displacements between approximately 0.4 and 1mm (which are the likely displacement values at weld bead crack initiation). This corresponds to the range of crack arrest toughness values normally found at temperatures around the CAT in large–scale, structurally representative tests (1,3). This result therefore suggests that the successful correlation between CAT and (NDTT +30°C) or (NDTT +40°C) is because the material has the same arrest toughness at these temperatures, as inferred from large–scale experiments and DWTs.

INSTRUMENTED 'PELLINI' DROP–WEIGHT TESTS

Instrumented drop–weight tests were carried out to obtain further information about the mechanics of this test. DWT specimens were instrumented with strain gauges on the tension face of the specimens on either side of the weld bead (Fig.1a). Tests were carried out at different rates of loading at temperatures between –65°C (measured NDTT), and 20°C (NDTT +85°C) using a servo–hydraulic testing machine. All but one of the static and one of the intermediate rate tests were carried out without using deflection stops to avoid damage to the strain gauges.

In the static (displacement rate = 0.17mm/s) tests, weld bead initiation took place at specimen displacements between 0.3 and 0.8mm, subject to some scatter. The specimen displacement was determined from the machine crosshead displacement, corrected for load train displacements. The results, together with an examination of the fracture faces revealed three types of crack extension behaviour: (i) propagation of a brittle crack to the limit of the weld bead HAZ then arrest; (ii) arrest at the limit of the weld bead HAZ, then extension by a stable ductile tearing mechanisms followed by re–initiation of a brittle crack and final arrest; and (iii) brittle propagation from the weld bead notch to the final arrested crack shape (cf. Fig.1b).

The static DWTs allowed the time/displacement when weld bead initiation took place to be determined and showed that an arrest/re-initiation event is a possible failure mechanism. A comparison of the displacement at initiation/arrest with the finite element analyses results, Fig.4, gives an estimate of the applied stress intensity factor at arrest (see Table 1). This is a 'greater than' estimate of the crack arrest toughness for a shallow flaw configuration.

TABLE 1 Effective stress intensity factor (K_J) in instrumented drop-weight specimens, determined from the measured displacement at weld bead initiation and the FEA results in Fig.4

Temperature, °C	Displacement rate, mm/s	Displacement at weld bead initiation and arrest, mm	K_J at deepest point of assumed crack, MPa√m
RT	0.167 (static)	0.64	105
RT		0.64	105
-30		0.45	77 (1)
-30		0.42	69 (1)
-65		0.78	121 (2)
-65		0.27	46 (1)
-25	500 (intermediate)	0.73	116
-25		0.94	141
-25		0.62	100

Notes: (1) Prior to re-initiation. (2) No arrest.

At -65°C, the crack did not arrest at the limit of the weld bead HAZ for one specimen, this means that the calculated applied stress intensity factor for this specimen exceeded the crack arrest toughness of the material. The second test resulted in arrest prior to re-initiation. The crack arrest toughness at -65°C for the steel investigated lies thus between 46 and 121MPa√m. The static results in Table 1 at RT and -30°C are 'greater than' results, since all tests resulted in arrest immediately after the crack emerged from the brittle weld bead. The intermediate rate (500mm/s) test results are included in Table 1. In all three specimens, the crack arrested after emerging from the brittle weld bead. The 'greater than' estimates of the crack arrest toughness for this specimen configuration exceeds 141MPa√m at -25°C.

CONCLUDING REMARKS

The finite element stress analysis of a drop-weight test specimen, containing a crack extending to the limit of the weld bead HAZ (which is representative of a specimen tested at approximately (NDTT +30°C) to (NDTT +40°C)), has shown that the applied effective stress intensity factor in the cracked drop-weight specimen lies between 70 and 150MPa√m (depending on the specimen displacement at weld bead initiation). This value compares very favourably with the crack arrest toughness normally measured in large-

scale tests at CAT. This results therefore provides an approximate confirmation of the correlation between CAT and (NDTT +30°C) to (NDTT +40°C).

Instrumented drop–weight tests can be carried out to determine the specimen displacement at the instant of crack initiation in the weld bead. Frequently the crack in a DWT specimen is arrested immediately after it emerges from the weld bead HAZ and re–initiates at later stages in the test. The specimen displacement value at arrest can be obtained with FEA results to determine approximate crack arrest toughness values at arrest.

Acknowledgement The results presented were obtained during the Group Sponsored Project "The 'Pellini' drop–weight test for crack arrest in modern steels". The financial support of its sponsors, British Gas plc, British Steel plc, Electricité de France, Fabrique de Fer Charleroi SA, Framatome, UK Health & Safety Executive and Shell International Petroleum Maatschappij BV is acknowledged gratefully.

REFERENCES

(1) Wiesner C S and Hayes B, "A review of crack arrest tests models and applications", Proc. Conf. 'Crack Arrest Concepts for Failure Prevention and Life Extension', Paper 2, Abington Publishing, 1996.

(2) ASTM E1221, "Standard test method for determining plane strain crack arrest toughness K_{Ia} of ferritic steels", American Society for Testing and Materials, 1991.

(3) Wiesner C S, Hayes B, Smith S D and Willoughby A A, Fat. Fract. Eng. Mat. Struct., Vol.17 (1994), 221–233.

(4) Wiesner C S, Hayes B and Willoughby A A, Int. J. Pres. Vess. & Pip., Vol.56 (1993), 369–385.

(5) Wiesner C S, Int. J. Pres. Vess. & Pip. (1996), in print.

(6) ASTM E208, "Standard test method for conducting drop–weight tests to determine nil–ductility transition temperature of ferritic steels", American Society of Testing and Materials, 1991.

(7) Wallin H, Planman T and Rintamaa R, "Comparison of some indirect measures of crack arrest", proc. Conf. 'Crack Arrest Concepts for Failure Prevention and Life Extension', Paper 7, Abington Publishing, 1996.

(8) Irwin G R, Krafft J M, Paris P C and Wells A A. "Basic aspects of crack growth and fracture", Report No. 6596, Naval Research Laboratory, Washington DC, 1967.

(9) Sumpter J D G, "Fracture mechanics interpretation of the drop–weight NDT temperature", ASTM STP 919, 1986, pp.142–160.

(10) Sreenivasan P R, Ray S K, Mannan S L and Rodriguez P, Int. J. Fra., Vol.55 (1992), pp.273–283

(11) ABAQUS (Version 5.3) User's Manual, Hibbit, Karlsson and Sorenson Inc., 1080 Main St., Pawtucket, RI, USA, 1993.

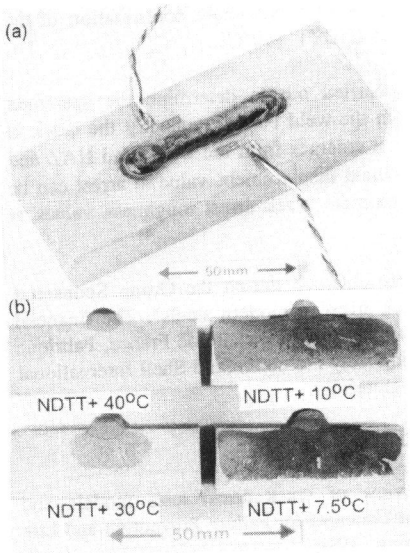

Fig.1 Drop-weight 'Pellini' specimen: (a) instrumentation (b) fracture face appearance of conventionally tested specimens

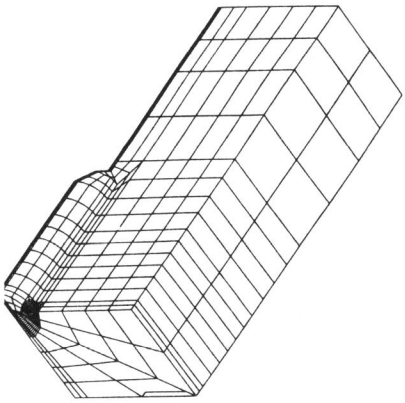

Fig.2 Three-dimensional FE mesh used in the analysis

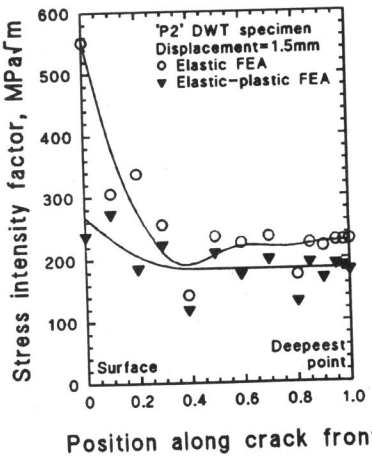

Fig.3 Elastic (K) and elastic-plastic (K_J) stress intensity factor along the assumed crack front (expressed in normalised distance from the tension face of the specimen)

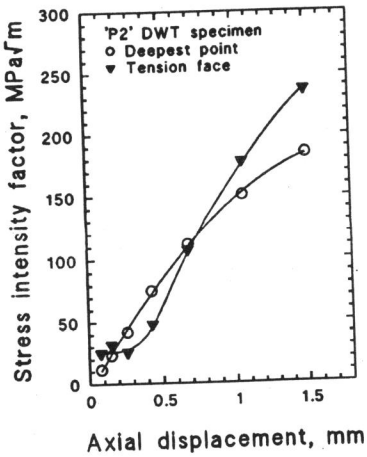

Fig.4 Elastic-plastic stress intensity factor K_J versus specimen displacement at the deepest point and the surface intersection of the crack